SAND2021-9958C

Supervisory Optimal Control for Photovoltaics Connected to an Electric Power Grid

Joseph Young
OptimoJoe
Houston, TX
Email: joe@optimojoe.com

Wayne Weaver
Michigan Technological University
Houghton, MI
Email: wwweaver@mtu.edu

David G. Wilson
Electrical Science and Experiments
Sandia National Laboratories
Albuquerque, NM
Email: dwilso@sandia.gov

Rush D. Robinett III
Michigan Technological University
Houghton, MI
Email: rdrobine@mtu.edu

***Abstract*—The following research presents an optimal control framework called Oxtimal that facilitates the efficient use and control of photovoltaic (PV) solar arrays. This framework consists of reduced order models (ROM) of photovoltaics and DC connection components connected to an electric power grid (EPG), a discretization of the resulting state equations using an orthogonal spline collocation method (OSCM), and an optimization driver to solve the resulting formulation. Once formulated, the framework is validated using realistic solar profiles and loads from actual residential applications.**

***Index Terms*—Microgrid, Solar, Photovoltaic, Control, Optimization**

I. Introduction

In the modern grid of today and the smart grid of tomorrow, reduced energy consumption and greater stability can be realized through the use of predictive control technology integrated with renewable energy. This approach leverages a combination of historical and real-time data to optimally synchronize green energy assets for balanced supply and demand. Simultaneously, microgrids are being used to improve reliability and resilience of electrical grids and manage the addition of distributed green energy resources like wind and solar photovoltaic (PV) generation, which helps reduce carbon-based generation dependency [1]. As a secondary benefit, microgrids also provide electricity to areas not served by centralized electrical infrastructure [1].

From a United States Department of Energy Office of Energy Efficiency and Renewable Energy (DOE EERE) perspective a reliable and secure energy grid that uses Distributed Energy Resources (DER) will be needed to ensure continuous electrical infrastructure that is independent of weather or unforeseen events [2]. DER examples for residences and businesses include rooftop solar panels, backup batteries, and emergency conventional generators [2]. Community-scale microgrids can also provide resiliency and backup during and after disasters such as hurricanes [2]. To manage risks associated with microgrid islanding and standalone applications improved control designs are needed for enhanced grid support and services.

Many researchers [3], [4], [5], [6], [7] have investigated advanced control techniques for microgrids. Nevertheless, the DC microgrid is still new in terms of grid architecture and control systems [8]. Within these microgrids, Energy Management Systems (EMS) are necessary for optimal use of DERs in a control structure with secure, reliable, and autonomous self-regulating functionality [8]. In addition, DC distribution systems are ideal for integrating DER and Energy Storage Systems (ESS) [9], [10], which are critical for the stability, reliability, and overall performance in a microgrid.

In this paper a fundamental EMS for DC microgrids in terms of ESS sizing and performance optimization is discussed. The fundamental framework relies on ROMs [11], [12] of residential PV, ESS, and DC power electronics that serves residential loads as part of a DC microgrid scenario summarized in Figure 1.

More specifically, the following paper describes a control framework for a residential PV microgrid that uses an optimal control algorithm based on an on-line optimization engine with a receding horizon control. The meaning and reason behind each of these characteristics is described below.

This control framework uses the term *optimal control* since the control results from the solution of an optimization formulation that minimizes certain criteria. Given the formulation is not convex, the control framework does not guarantee a global minima, but given sufficient time it can guarantee a local minima. In practice, this minima is acceptable for control.

Even though this approach lacks a real-time guarantee, it may still be used as an on-line control. In an *on-line control*, the control framework repeatedly solves the control problem on a running system over a specified time horizon. This differs from an *off-line control*, which solves the control problem for a system not in operation. Although an on-line control requires a prediction of the future, as long as the inputs to the system can be predicted sufficiently well, it can provide a useful control. Suh and Choi [13] provide an overview of modern methods and software for estimating electric power production from PV systems. The NREL code System Advisor Model (SAM) [14], [15] is an example of a piece of software that provides these predictions.

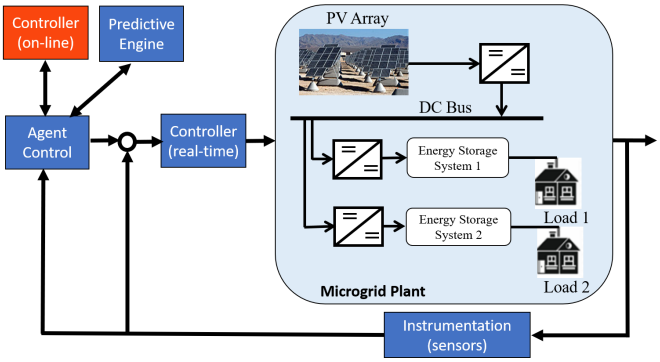

Fig. 1. Overall control architecture

In order to make the process of prediction and control more robust, this control framework employs a *receding-horizon control*, which is also known as a *model-predictive control*. In a receding-horizon control, the inputs that characterize the system are predicted over a specified time horizon and then a control over this time period is found. This time period is known as the *planning horizon*. If the actual inputs to the system differ too far from this prediction, the previously solved control is discarded and a new control is determined. This shorter time window is called the *execution horizon*.

Since an on-line control does not provide run-time guarantees, this kind of control is generally used for medium to long-term planning. For short-term control, an on-line control is typically combined with a real-time control that moderates rapidly changing dynamics.

The coordination between the different controls can be accomplished through the use of *software agents* located throughout the power system architecture. Software agents monitor the state of the system through the use of sensors, determine the appropriate course of action, and then influence the system behavior by advising the different controllers. The use of software agents for power system control continues to evolve. Recently, there has been emphasis on single agent control strategies coupled with team level strategies [16]. Wilson et al. describe one such methodology for combining these controllers [17] and a simplified diagram of how these components interconnect can be found in Figure 1. While these interactions are important, this paper focuses on the longer term plan through the use of the optimal control used by the on-line control.

The methodology presented in this paper can be compared to the techniques used by a variety of different teams. Park et al. studied the use of a model predictive control for shipboard power management systems [18]. There, the authors use an integrated perturbation analysis and sequential quadratic programming (IPA-SQP) solver from Ghaemi, Sun, and Kolmanovsky [19] to find a control that determines how power is used within the system. The framework presented here differs from Park et al. in that their work attempts to find a real time controller, but sacrifices optimality in the case where the perturbation in the initial conditions is too large. The framework under discussion finds an optimal solution, but provides no real-time guarantees and must be used on-line. Both methodologies also differ in the reduced-order model used for their respective analyses.

Abhinav et al. [20] present an optimization strategy for the frequency synchronization of multiple AC microgrids. In their approach, they formulate the control as a convex optimization problem, which they then solve using the Alternative Directional Multiple of Multipliers (ADMM). The framework here differs from their approach in that their work focuses on synchronization of AC microgrids and this framework focuses on the overall operation of DC microgrids. Next, their work uses distributed optimization algorithms whereas this framework uses a parallel, nonlinear optimization solver. In addition, while both methodologies use a circuit based reduced order model, they differ in the actual model used.

The framework described in this document improves upon the reduced order model, discretization, and optimization used by Wilson et al. [21], [22], [17], Young, Cook, and Wilson [23], Weaver et al. [11], and Hassel et al. [12]. In this paper, the reduced order model of the electrical microgrid is both simplified and generalized by combining the microgrid components into an alternating sequence of series and parallel circuit components that represent the power system. Next, the discretization is improved from a finite difference method to an orthogonal spline collocation method. This allows for improved model fidelity and state control. Finally, this resulting formulation is solved using faster, more powerful algorithms from a prototype version of Optizelle [24], which implements an inexact composite-step SQP method combined with a primal-dual interior point method. This allows the model fidelity to be improved by over an order of magnitude. Nevertheless, the formulation is generic and other nonlinear optimization algorithms and software can be applied. However, their performance is not examined here.

This current approach to control was first described in a paper by Young, Wilson, and Cook [25]. This paper improves upon and differs from that work in two key respects. First, it changes the application from a shipboard power system to a residential PV application in an effort to demonstrate the broadly applicable nature of the reduced-order model as well as the control framework. Second, it presents and demonstrates how nonlinear bounds can be implemented and applied to the state variables within the control formulation. This last feature is somewhat unusual for an optimal control due to the difficulty in implementing such a feature in a more traditional differential equation solver such as a Runge-Kutta method.

Finally, this work is being presented in conjunction with a separate paper from Young, Wilson, Weaver, and Robinett [26] that details a similar approach to the control of wind turbines. Though related, these two papers differ in the reduced-order models used and objective sought by the optimal control formulation.

The paper is divided into six sections. In Section II, the paper introduces the reduced order model used to represent the microgrid. In order to discretize these equations, Section III describes the orthogonal spline collocation method. Using the fully discretized dynamics, Section IV formulates the optimal control. Then, using the completed framework,

Section V describes the application of the optimal control to a small DC solar microgrid scenario. Finally, Section VI summarizes the paper's findings.

II. Reduced Order Model

To model an electrical microgrid, this control framework represents the microgrid as a circuit using Kirchoff's circuit laws. Similar to the work of Wilson et al. [21], [22], [17] and Young, Cook, and Wilson [23], [25], the model is comprised of an alternating sequence of series DC circuits in Figure 2 or parallel DC circuits in Figure 3. In these diagrams, components outlined in dotted squares are optional.

In this reduced order model, power generation is represented as either a constant current source in a parallel DC component or as a constant voltage source in a series DC component. In the series components, the variable λ denotes the duty cycle in an average-mode model of a boost/buck converter. Only one such switch occurs in an individual component and its location depends on the voltage difference between the source and sink. As far as storage, it is represented using the variable u and is present either as a voltage source in a series DC component or a as a current source in a parallel DC component. In the parallel DC component, the variable P represents a direct power load that removes a specified amount of power from the system, which models the load from a given device. In a similar manner, d represents a kind of *dispatchable load*. Like P, it removes power from the system, but the controller is given the ability to softly meet a load demand, D. This means that the control may provide more or less power at any particular instance with the overall goal of providing the same amount of energy over the entire planning horizon. When possible, the original load profile is followed. In terms of connectivity, the parallel DC component may accept any number of sources and sinks whereas the series DC component contains a single source and a single sink.

Using these components, the state dynamics for the series DC components are represented as

$$[\lambda]v_{src} + [u] = Li' + Ri + [\lambda]v_{snk} \tag{1}$$
$$i(0) = i_0 \tag{2}$$
$$i_{\min} \leq i \leq i_{\max} \tag{3}$$
$$w' = -ui \tag{4}$$
$$w(0) = w_0 \tag{5}$$
$$0 \leq w \leq w_{\max} \tag{6}$$
$$0 \leq \lambda \leq 1 \tag{7}$$

and the parallel DC components as

$$\sum[\lambda_{src}]i_{src} + [u] = \sum[\lambda_{snk}]i_{snk} + Cv' + \tfrac{v}{R} + \left[\tfrac{P}{v}\right] + \left[\tfrac{d}{v}\right] \tag{8}$$
$$v = \text{const} \tag{9}$$
$$w' = -vu \tag{10}$$
$$w(0) = w_0 \tag{11}$$
$$0 \leq w \leq w_{\max} \tag{12}$$
$$0 \leq d. \tag{13}$$

In these equations and bounds, square brackets denote elements that may be present or not present depending on the configuration of the grid. As a note for the DC parallel component, since the control framework holds v constant, the capacitor C becomes vestigial and the resulting formulation becomes a differential algebraic equation (DAE.) As a result, holding v constant does create some difficulty since the resulting system may not necessarily be feasible without enough fidelity in the available controls. Most often, this can be ensured by requiring that there exist more control than state variables after discretization modulo bounds on the control variables.

In summary, the control framework employs a reduced order model comprised of an alternating sequence of parallel and series circuits. These components are highly configurable and allow a microgrid that contain a various assortment of generation, loads, voltages, and storage devices to be quickly assembled.

III. Discretization

In order to satisfy the dynamics described in the previous section, the control framework uses an Orthogonal Spline Collocation Method (OSCM.) Properties of this approach are described by de Boor and Swartz in [27]. In short, an OSCM represents each unknown function as a Hermite cubic spline with unknown coefficients. These coefficients become the variables in the optimization formulation. The polynomials that constitute these splines are given by

$$h_{00}(t) = (1+2t)(1-t)^2 \tag{14}$$
$$h_{10}(t) = t(1-t)^2 \tag{15}$$
$$h_{01}(t) = t^2(3-2t) \tag{16}$$
$$h_{11}(t) = t^2(t-1). \tag{17}$$

Then, the control framework attempts to satisfy the dynamics at specified points called collocation points. When the collocation points correspond to Gaussian quadrature points, the OSCM converges to the true solution of the DAE at the rate $O(h^4)$ where h denotes the largest interval in the mesh used by the Hermite cubic spline.

In order to assemble the system of equations required for optimization, the control framework employs an assembly scheme similar to the one used by older versions of Chebfun [28], [29]. It accomplishes this by creating and utilizing a combination of evaluation operators, E, and differentiation operators, D, that map the coefficients of a Hermite cubic spline to the evaluation of that spline, or its derivative, at the collocation points defined by the spline's mesh. In other words, the domain of these operators is the space of coefficients of the spline and the codomain is either the evaluation or derivative at the collocation points. For example, the differential equation

$$u' = -u \tag{18}$$

is discretized as

$$D\alpha = -E\alpha \tag{19}$$

where α represents the coefficients of the spline. Note, this example does not impose boundary conditions, but these can be enforced using a similar methodology. As a note, while Chebyshev polynomials generally provide a superior approximation and model fidelity, Hermite cubic splines

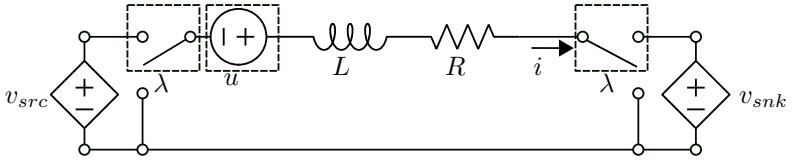

Fig. 2. Series DC Component

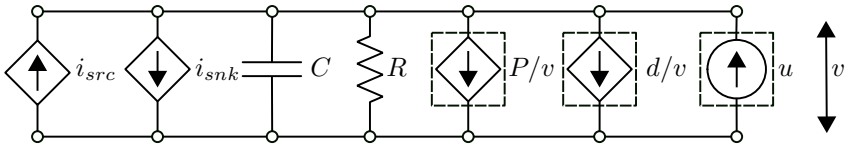

Fig. 3. Parallel DC Component

possess a number of desirable properties that are utilized by this control framework.

As shown by Carlson and Fritsch [30], the control framework can bound the values of a Hermite cubic spline over the entire domain by bounding the coefficients. Succinctly, the Hermite polynomial

$$p(t) = \alpha_1 h_{00}(t) + \alpha_2 h_{10}(t) + \alpha_3 h_{01}(t) + \alpha_4 h_{11}(t) \quad (20)$$

is bounded between l and u on the interval $[0, 1]$ whenever the following inequalities are satisfied

$$3l \leq 3\alpha_1 + \alpha_2 \leq 3u \quad (21)$$
$$3l \leq 3\alpha_1 - \alpha_2 \leq 3u \quad (22)$$
$$3l \leq 3\alpha_3 + \alpha_4 \leq 3u \quad (23)$$
$$3l \leq 3\alpha_3 - \alpha_4 \leq 3u. \quad (24)$$

If an upper or lower bound is undesired, simply remove that side of the inequality. Note, this approach not only allows the control variables to be bounded, but the state as well. Further, these bounds are satisfied over the entire domain and not just at the collocation or mesh points. This ensures that certain values, such as the overall power output of a generator or the capacity of a storage device, are never exceeded.

These bounds can be extended to nonlinear functions as well. To bound the Hermite polynomial p by the Hermite polynomials l,

$$l(t) = l_1 h_{00}(t) + l_2 h_{10}(t) + l_3 h_{01}(t) + l_4 h_{11}(t), \quad (25)$$

and u,

$$u(t) = u_1 h_{00}(t) + u_2 h_{10}(t) + u_3 h_{01}(t) + u_4 h_{11}(t), \quad (26)$$

a similar bound can be used,

$$3l_1 + l_2 \leq 3\alpha_1 + \alpha_2 \leq 3u_1 + u_2 \quad (27)$$
$$3l_1 - l_2 \leq 3\alpha_1 - \alpha_2 \leq 3u_1 - u_2 \quad (28)$$
$$3l_3 + l_4 \leq 3\alpha_3 + \alpha_4 \leq 3u_3 + u_4 \quad (29)$$
$$3l_3 - l_4 \leq 3\alpha_3 - \alpha_4 \leq 3u_3 - u_4. \quad (30)$$

As a result, if a nonlinear bound can be represented by a Hermite cubic spline on the same mesh as the bounded state or control variable, then it can be bounded over the entire domain.

One additional benefit of using Gaussian quadrature points as collocation points is that a spline can be quickly integrated. Specifically, given the mesh $\Omega = (t_0, \ldots, t_{\text{nele}})$, spline s, and collocation points C, then

$$\int_{t_0}^{t_{\text{nele}}} s(t)dt = \sum_{k=0}^{\text{nele}-1} (t_{k+1} - t_k)(s(C_{2k+1}) + s(C_{2k+2})). \quad (31)$$

In summary, the OSCM provides a tool that allows the discretization of the reduced order model of the microgrid. It is numerically stable, sparse, allows both differentiation and integration of its quantities, and can be bounded over the entire domain.

IV. Optimal Control Formulation

In order to specify the behavior of the control, this framework focuses on two different objectives. First, the framework provides the ability to limit the use of storage necessary to satisfy the dynamics of the grid. Second, the framework gives the ability to limit the deviation of the dispatchable loads from their desired usage.

With respect to the storage, some scenarios require the storage devices to remain discharged and others require them to remain charged. To accommodate each of these cases, it uses the objective

$$\min \int_0^{t_{\text{end}}} (w_{\text{trg}} - w(t))^2 dt \quad (32)$$

where w_{trg} represents the target amount of energy in the storage device. If a discharged storage device is requested, this is zero, and if a charged device is required, this is $w_{\max}$. Note, the discretization techniques described above provide a fast methodology to compute these integrals.

In order to match the actual dispatchable load to the desired, two different objects are used. First, in order to match the shape over time, the framework minimizes the integral of the difference between the desired load D and the actual load d squared

$$\min \int_0^{t_{\text{end}}} (d(t) - D(t))^2 dt. \quad (33)$$

This objective penalizes the deviation at any point in time. Second, to match the overall energy expenditure from the dispatchable load, the framework minimizes the square of the integral of the difference between D and d

$$\min \left(\int_0^{t_{\text{end}}} d(t) - D(t) \right)^2 dt. \quad (34)$$

This allows the electrical microgrid to catch back up to an overall state in case it needed to divert power elsewhere.

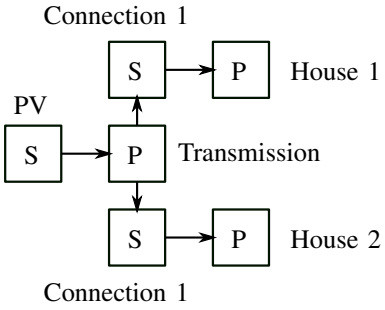

Fig. 4. Residential PV microgrid. P denotes a parallel component and S denotes a series component. Base of the arrow denotes a source and the point a sink.

Generally speaking, matching the overall energy expenditure is more important than matching the shape, so the expenditure objectives should be weighted higher than the shape objectives.

Putting this all together, the optimal control formulation becomes

Minimize	Use of storage devices
	Deviation from dispatchable load
Subject to	Series DC component dynamics
	Parallel DC component dynamics

Note, any combination of the above objectives and their weighting can be used.

To solve the above formulation, the control uses a prototype version of Optizelle [24], which implements a modified version of the composite step SQP method developed by Ridzal and Heinkenschloss [31], [32], [33]. This is combined with a primal-dual interior point method in a manner similar to NITRO described by Byrd, Hribar, and Nocedal [34]. The augmented systems that arise from this formulation are solved using a Q-less QR factorization developed by Davis [35].

V. Computational Results

In order to validate the control framework, consider a reduced order model of a small DC microgrid consisting of a single PV array shared between two houses described by the topology in Figure 4. The components in this reduced order model correspond to the components in Figures 2 and 3. Within these components, the following parameters are used

1) PV voltage, v_{src} - 110 V
2) PV sink, v_{snk} - Transmission
3) PV inductance, L - 0.001 H
4) PV resistance, R - 0.121 Ω, which gives a parasitic loss of 250 W at max generation
5) PV minimum current, $i_{\min}$ - 0 A
6) PV maximum current, $i_{\max}$ - Nonlinear function determined by the NREL code System Advisor Model (SAM) [14], [15] based on 5 kW max generation using averaged historical weather information for Albuquerque, NM on a typical May 1
7) Transmission source, i_{src} - PV
8) Transmission sink, i_{snk} - Connection 1 and 2
9) Transmission voltage, v - 200 V
10) Transmission resistance, R - 160 Ω, which gives a parasitic loss of 250 W
11) Connection source, v_{src} - Transmission
12) Connection sink, v_{snk} - House 1 or 2
13) Connection inductance, L - 0.001 H
14) Connection resistance, R - 0.05 Ω
15) House source, i_{src} - Connection 1 or 2
16) House voltage, v - 220 V
17) House storage, $w_{\max}$ - House 1 contains 3 MJ (0.83 kW h) of storage whereas House 2 contains 4 MJ (1.11 kW h) of storage. The storage uses two different capacities to improve the visibility of the plots.
18) House load, P - Nonlinear function derived from load profiles determined by sampling loads from two separate houses located in Albuquerque, NM
19) House dispatchable load, D - No dispatchable load, but potentially useful here to model smart devices that can shed load when demand is exceptionally high
20) House resistance, R - 193.6 Ω - Parasitic loss of 250 W

As far as the discretization, the control framework solves for a control that lasts 9 h (0700-1600) using a discretization with 2161 elements. This gives a mesh with node boundaries every 15 s and results in an optimization formulation that contains 86440 constraints and 95084 variables.

In terms of the objective, the control framework attempts to keep the energy storage devices at 90% charge. The purpose of this objective is to keep the storage devices mostly charged while preserving their ability to assist in the operation of the grid by either storing or delivering power.

The load demands can be seen in Figure 5. To handle these load demands and refill any energy storage devices, the grid uses the amount of power in Figure 6. Note, the difference between the amount of generation and the maximum amount of generation represents unused power that could be potentially redistributed to a municipal power grid. The amount of energy stored in each house can be seen in Figure 8. Recall, the goal is to keep the energy storage devices at 90% charge and not use them when not required. Here, the control meets this goal and only uses the storage in the morning when demand exceeds supply. In order to bring this power to the appropriate loads, the grid transfers power from one component to another. The duty cycles associated with the changes in voltage during this transfer can be seen in Figure 7.

For a closer look at a portion of the scenario from 0830-1030, consider Figures 9, 10, and 11. Here it can be more easily seen how the storage is used to meet load demand.

VI. Conclusions

The preceding document describes a framework for the optimal control of an electrical microgrid powered by a PV array.

The control framework consists of a reduced-order model of an electric microgrid comprised of a collection of series and parallel circuit components, a discretization based on an orthogonal spline collocation method, and an optimization engine used to solve the resulting formulation.

To validate the control framework, it is applied to a small residential power grid using a combination of historical weather information and actual loads. The resulting control

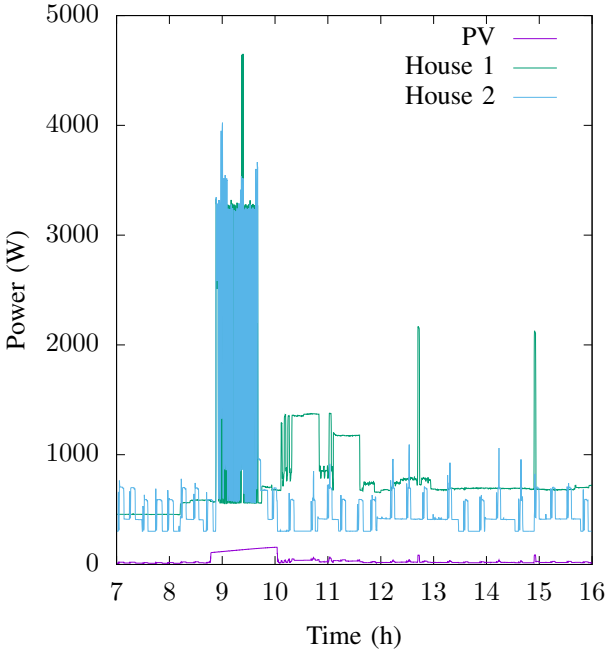

Fig. 5. Load power

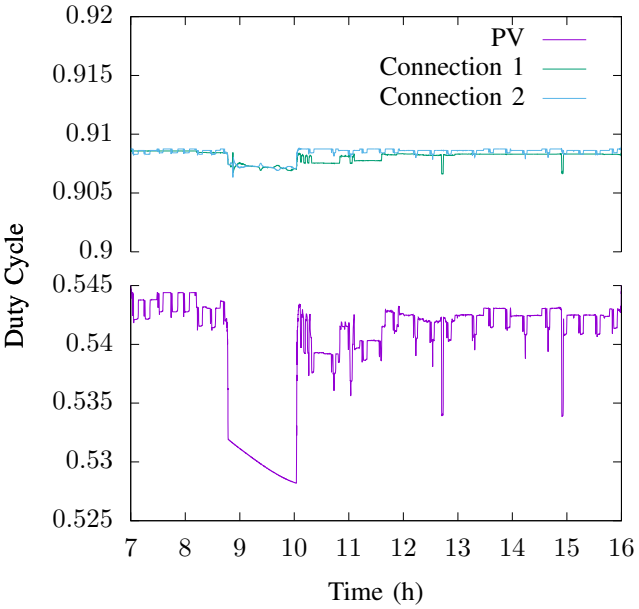

Fig. 7. Boost converter duty cycles

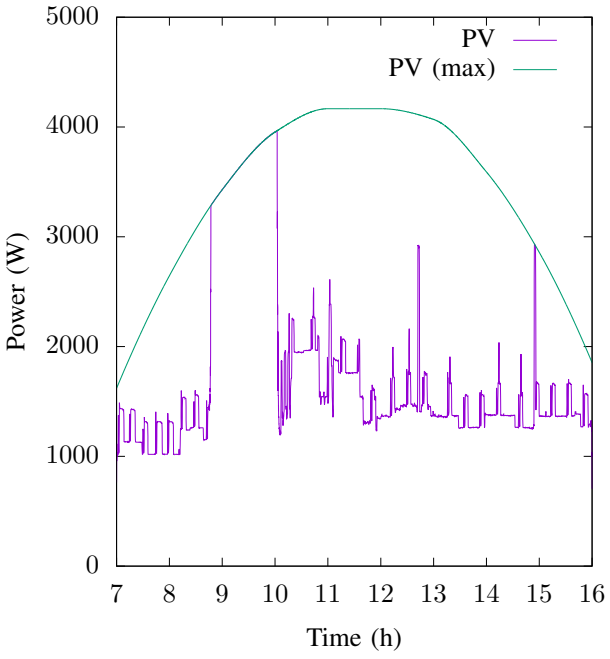

Fig. 6. Power generation versus maximum power generation. Difference between the two represents unused generation capacity.

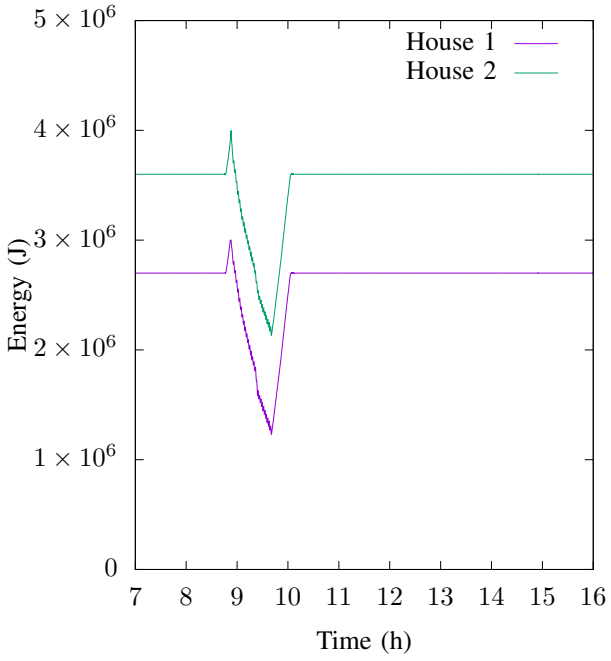

Fig. 8. Stored energy

demonstrates that the use of storage devices can be minimized through the effective coordination.

In the future, this work can be extended to work on alternative scenarios of interest as well as incorporate AC modules.

ACKNOWLEDGMENT

This study was funded by the Laboratory Directed Research & Development (LDRD) program at Sandia National Laboratories. Sandia National Laboratories is a multi-mission laboratory managed and operated by National Technology and Engineering Solutions of Sandia, LLC., a wholly owned subsidiary of Honeywell International, Inc., for the U.S. Department of Energy's National Nuclear Security Administration under contract DE-NA0003525. This paper describes objective technical results and analysis. Any subjective views or opinions that might be expressed in the paper do not necessarily represent the views of the U.S. Department of Energy or the United States Government. Special thanks to Dr. Ray Byrne at Sandia, for his technical

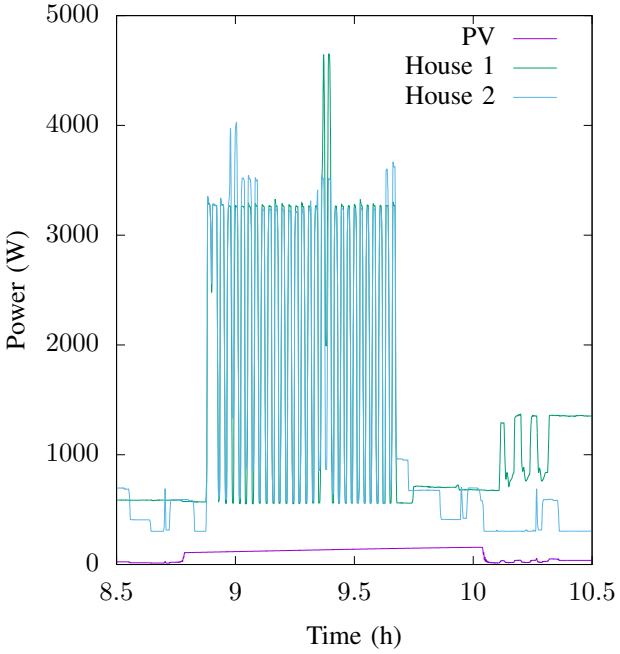

Fig. 9. Excerpt of the load power on a shorter time interval

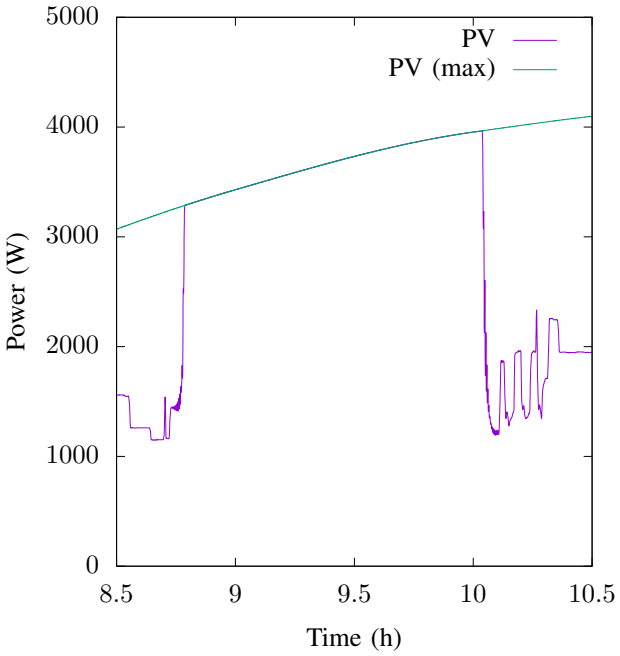

Fig. 10. Excerpt of the power generation on a shorter time interval. Note, actual generation is successfully bounded and never exceeds the maximum possible generation.

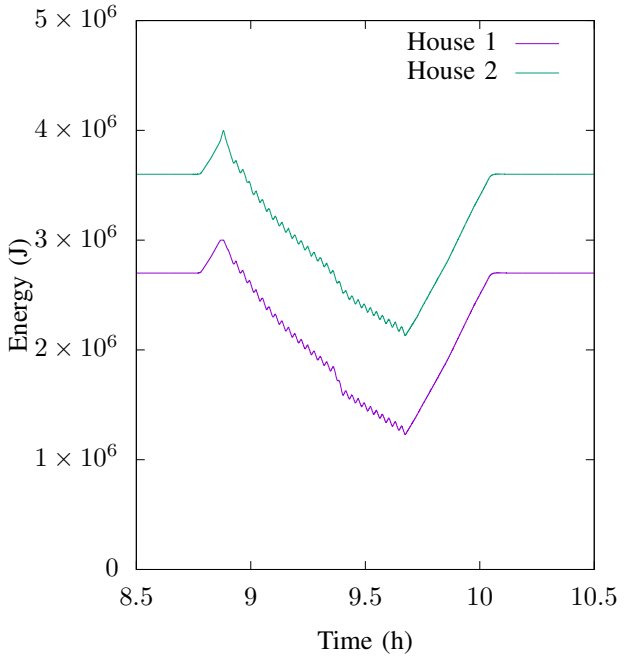

Fig. 11. Excerpt of the stored energy on a shorter time interval

review and programmatic leadership for this LDRD project. This paper approved as SAND2021-XXXXC.

References

[1] A. Hirsch, Y. Parag, and J. Guerrero, "Microgrids: A review of technologies, key drivers, and outstanding issues," *Renewable and Sustainable Energy Reviews*, vol. 90, pp. 402–411, 2018. [Online]. Available: https://www.sciencedirect.com/science/article/pii/S136403211830128X

[2] "Solar integration: Distributed energy resources and microgrids," https://www.energy.gov/eere/solar/solar-integration-distributed-energy-resources-and-microgrids, accessed: 2021-08-11.

[3] A. H. Etemadi, E. J. Davison, and R. Iravani, "A decentralized robust control strategy for multi-der microgrids-part i: Fundamental concepts," *IEEE Transactions on Power Delivery*, vol. 27, no. 4, pp. 1843–1853, 2012.

[4] J. Rocabert, A. Luna, F. Blaabjerg, and P. Rodrguez, "Control of power converters in ac microgrids," *IEEE Transactions on Power Electronics*, vol. 27, no. 11, pp. 4734–4749, 2012.

[5] A. H. Etemadi, E. J. Davison, and R. Iravani, "A generalized decentralized robust control of islanded microgrids," *IEEE Transactions on Power Systems*, vol. 29, no. 6, pp. 3102–3113, 2014.

[6] M. D. Cook, G. G. Parker, R. D. Robinett, and W. W. Weaver, "Decentralized mode-adaptive guidance and control for dc microgrid," *IEEE Transactions on Power Delivery*, vol. 32, no. 1, pp. 263–271, 2017.

[7] M. Toub, R. D. Robinett, M. Maaroufi, and G. Aniba, "Decentralized hamiltonian control of multi-der isolated microgrids with meshed topology," *Energy Procedia*, vol. 157, pp. 1253–1265, 01 2019.

[8] S. Ali, Z. Zheng, M. Aillerie, J.-P. Sawicki, M.-C. Pra, and D. Hissel, "A review of dc microgrid energy management systems dedicated to residential applications," *Energies*, vol. 14, no. 14, 2021. [Online]. Available: https://www.mdpi.com/1996-1073/14/14/4308

[9] M. B. Shadmand and R. S. Balog, "Multi-objective optimization and design of photovoltaic-wind hybrid system for community smart dc microgrid," *IEEE Transactions on Smart Grid*, vol. 5, no. 5, pp. 2635–2643, 2014.

[10] B. Wang, M. Sechilariu, and F. Locment, "Intelligent dc microgrid with smart grid communications: Control strategy consideration and design," *IEEE Transactions on Smart Grid*, vol. 3, no. 4, pp. 2148–2156, 2012.

[11] W. W. Weaver, R. D. Robinett, G. G. Parker, and D. G. Wilson, "Distributed control and energy storage requirements of networked dc microgrids," *Control Engineering*

Practice, vol. 44, pp. 10–19, 2015. [Online]. Available: https://www.sciencedirect.com/science/article/pii/S0967066115001185

[12] T. Hassell, W. W. Weaver, R. D. Robinett, D. G. Wilson, and G. G. Parker, "Modeling of inverter based ac microgrids for control development," in *2015 IEEE Conference on Control Applications (CCA)*, 2015, pp. 1347–1353.

[13] J. Suh and Y. Choi, "Methods for converting monthly total irradiance data into hourly data to estimate electric power production from photovoltaic systems: A comparative study," *Sustainability*, vol. 9, no. 7, 2017. [Online]. Available: https://www.mdpi.com/2071-1050/9/7/1234

[14] NREL, "System advisor model version 2020.11.29 (sam 2020.11.29)," https://sam.nrel.gov, 2020.

[15] N. Blair, N. DiOrio, J. Freeman, P. Gilman, S. Janzou, T. Neises, and M. Wagner, "System advisor model (sam) general description (version 2017.9.5)," NREL, Tech. Rep. NREL/TP-6A20-70414, 2018.

[16] M. H. Moradi, S. Razini, and S. Mahdi Hosseinian, "State of art of multiagent systems in power engineering: A review," *Renewable and Sustainable Energy Reviews*, vol. 58, pp. 814–824, 2016. [Online]. Available: https://www.sciencedirect.com/science/article/pii/S1364032115017220

[17] D. G. Wilson, W. Weaver, R. D. Robinett, J. Young, S. F. Glover, M. A. Cook, S. Markle, and T. J. McCoy, "Nonlinear Power Flow Control Design Methodology for Navy Electric Ship Microgrid Energy Storage Requirements," in *14th International Naval Engineering Conference & Exhibition*, 2018, pp. 1–15.

[18] H. Park, J. Sun, S. Pekarek, P. Stone, D. Opila, R. Meyer, I. Kolmanovsky, and R. DeCarlo, "Real-time model predictive control for shipboard power management using the IPA-SQP approach," *IEEE Transactions on Control Systems Technology*, vol. 23, no. 6, pp. 2129–2143, Nov 2015.

[19] R. Ghaemi, J. Sun, and I. V. Kolmanovsky, "An integrated perturbation analysis and sequential quadratic programming approach for model predictive control," *Automatica*, vol. 45, no. 10, pp. 2412 – 2418, 2009.

[20] S. Abhinav, I. D. Schizas, F. Ferrese, and A. Davoudi, "Optimization-based ac microgrid synchronization," *IEEE Transactions on Industrial Informatics*, vol. 13, no. 5, pp. 2339–2349, 2017.

[21] D. G. Wilson, J. C. Neely, M. A. Cook, S. F. Glover, J. Young, and R. D. Robinett, "Hamiltonian control design for dc microgrids with stochastic sources and loads with applications," in *2014 International*

[32] D. Ridzal, M. Aguiló, and M. Heinkenschloss, "Numerical study of matrix-free trust-region SQP method for equality constrained optimization," Sandia National Laboratories, Tech. Rep. SAND2011-9346, 2011.

Symposium on Power Electronics, Electrical Drives, Automation and Motion, June 2014, pp. 1264–1271.

[22] D. G. Wilson, R. D. Robinett, W. W. Weaver, R. H. Byrne, and J. Young, "Nonlinear power flow control design of high penetration renewable sources for ac inverter based microgrids," in *2016 International Symposium on Power Electronics, Electrical Drives, Automation and Motion (SPEEDAM)*, June 2016, pp. 701–708.

[23] J. Young, M. A. Cook, and D. G. Wilson, "A predictive engine for on-line optimal microgrid control," in *2017 IEEE Electric Ship Technologies Symposium (ESTS)*, 2017, pp. 564–571.

[24] J. Young, "Optizelle – an open source software library designed to solve general purpose nonlinear optimization problems," www.optimojoe.com, 2013–2021.

[25] J. Young, D. G. Wilson, and M. A. Cook, "The optimal control of an electric warship driven by an operational vignette," in *2021 IEEE Electric Ship Technologies Symposium (ESTS)*, 2021, To appear.

[26] J. Young, D. G. Wilson, W. Weaver, and R. D. Robinett, "The optimal control of type-4 wind turbines connected to an electric microgrid," in *20th Wind Integration Workshop*, 2021, To appear.

[27] C. de Boor and B. Swartz, "Collocation at gaussian points," *SIAM Journal on Numerical Analysis*, vol. 10, no. 4, pp. 582–606, 1973. [Online]. Available: https://doi.org/10.1137/0710052

[28] T. A. Driscoll, N. Hale, and L. N. Trefethen, *Chebfun Guide*. Pafnuty Publications, 2014. [Online]. Available: http://www.chebfun.org/docs/guide/

[29] L. N. Trefethen, *Spectral Methods in MatLab*. USA: Society for Industrial and Applied Mathematics, 2000.

[30] R. E. Carlson and F. N. Fritsch, "Monotone piecewise bicubic interpolation," *SIAM Journal on Numerical Analysis*, vol. 22, no. 2, pp. 386–400, 1985. [Online]. Available: https://doi.org/10.1137/0722023

[31] D. Ridzal, "Trust-region SQP methods with inexact linear system solves for large-scale optimization," Ph.D. dissertation, Rice University, 2006.

[33] M. Heinkenschloss and D. Ridzal, "A matrix-free trust-region sqp method for equality constrained optimization," *SIAM Journal on Optimization*, vol. 24, no. 3, pp. 1507–1541, 2014.

[34] R. H. Byrd, M. E. Hribar, and J. Nocedal, "An interior point algorithm for large-scale nonlinear programming," *SIAM Journal on Optimization*, vol. 9, no. 4, pp. 877–900, 1999.

[35] T. A. Davis, "Algorithm 915, suitesparseqr: Multifrontal multithreaded rank-revealing sparse QR factorization," *ACM Trans. Math. Softw.*, vol. 38, no. 1, Dec. 2011. [Online]. Available: https://doi.org/10.1145/2049662.2049670